The Rovibrational Intensities of Five Absorption Bands of $^{12}C^{16}O_2$ between 5218 and 5349 cm^{-1}

Lawrence P. Giver

Atmospheric Physics Branch, N 245-4

NASA Ames Research Center

Moffett Field, CA 94035-1000.

Linda R. Brown

Jet Propulsion Laboratory; California Institute of Technology

4800 Oak Grove Drive; Pasadena, CA 91109.

Charles Chackerian, Jr.

SETI Institute

Mountain View, CA 94043

and

Richard S. Freedman

Space Physics Research Institue

Sunnyvale, CA 94087

Number of pages: 28

Number of figures: 5

Number of tables: 9

Corresponding Author:

Lawrence P. Giver

Atmospheric Physics Branch; SGP, N 245-4.

NASA - Ames Research Center

Moffett Field, CA 94035-1000

Phone: (650) 604-5231

E-mail: lgiver@mail.arc.nasa.gov

ABSTRACT

Absolute line intensities, band intensities, and Herman-Wallis parameters were measured for the $(01^12)_I \leftarrow (00^00)_I$ perpendicular band of $^{12}C^{16}O_2$ centered at 5315 cm^{-1}, along with the three nearby associated hot bands: $(10^02)_{II} \leftarrow (01^10)_I$ at 5248 cm^{-1}, $(02^22)_I \leftarrow (01^10)_I$ at 5291 cm^{-1}, and $(10^02)_I \leftarrow (01^10)_I$ at 5349 cm^{-1}. The nearby parallel hot band $(30^01)_I \leftarrow (10^00)_{II}$ at 5218 cm^{-1} was also included in this study.

The rotationless band intensities at 296 K are respectively

Band	S^0_v $cm^{-1}/(molecule/cm^2)$
$(01^12)_I \leftarrow (00^00)_I$	$(47.6 \pm 0.4)\times10^{-24}$
$(10^02)_{II} \leftarrow (01^10)_I$	$(1.45 \pm 0.04)\times10^{-24}$
$(02^22)_I \leftarrow (01^10)_I$	$(3.60 \pm 0.05)\times10^{-24}$
$(10^02)_I \leftarrow (01^10)_I$	$(0.556 \pm 0.027)\times10^{-24}$
$(30^01)_I \leftarrow (10^00)_{II}$	$(2.279 \pm 0.031)\times10^{-24}$

INTRODUCTION

Modeling spectra of the near-infrared emission windows found on the nightside of Venus was undertaken by Pollack *et al.* [1] in an effort to improve the determination of the composition and cloud structure of the lower atmosphere of Venus. Since CO_2 is the most abundant gas in Venus' dense, hot atmosphere, weak overtone-combination bands and hot bands of CO_2 are ubiquitous throughout Venus' near-infrared spectrum. The intensities of many of these bands that are significant absorbers in Venus' atmosphere have not been measured; modeling Venus' spectrum must rely on calculated intensities for these bands. To improve this modeling work, Giver and Chackerian [2] made laboratory measurements of the intensity and Herman-Wallis parameters of the very weak $(31^10)_{IV}\leftarrow(00^00)$ perpendicular band of CO_2 at 4416 cm^{-1}, which is prominent in Venus' emission window between 4040 and 4550 cm^{-1}. Giver *et al.* [3] subsequently measured intensity parameters of two bands of the $(40^01)\leftarrow(00^00)$ pentad to help improve reliability of the modeling of the Venus emission window centered at 7830 cm^{-1}. Before these measurements, only calculated intensity parameters were available for simulating these CO_2 bands in atmospheric models.

The modeling of Pollack *et al.* [1] did not obtain a good fit to the 7830 cm^{-1} Venus emission window. As mentioned by Giver *et al.* [3], the very weak and perturbed $(21^12)_{II}\leftarrow(00^00)$ perpendicular band at 7901 cm^{-1} contributes some absorption on one side of the 7830 cm^{-1} Venus emission window. They measured the intensities of some Q- and R-branch lines of this band, but because of the perturbation and the lack of measurable P- branch lines, they did not obtain band intensity parameters. Rothman *et al.* [4] revised the intensity parameters of most of the unmeasured CO_2 bands for the 1992 HITRAN compilation using the Direct Numerical Diagonalization calculations of Wattson and Rothman [5], but they did not do that for this band or the other perturbed bands. Thus, the modeling calculations depended on the original McClatchey *et al.* [6] HITRAN

intensity estimate for this band, which has not been updated yet by either measurements or calculations.

The 1992 HITRAN values for the entire sequence of $(n1^12)\leftarrow(00^00)$ perpendicular bands and some of their associated hot bands are compared in Table 1 to the 1986 HITRAN values of Rothman [7], which were unchanged from the McClatchey *et al.* [6] estimates. There is a striking reduction for the calculated intensity of the $(01^12)_I\leftarrow(00^00)_I$ band at 5315.7 cm^{-1} from the 1986 to the 1992 HITRAN tabulation. However, it was recognized that the DND calculated intensities for this sequence of perpendicular bands may have substantial uncertainties, since none of the measured band intensities used by Wattson and Rothman [5] to determine the dipole-moment surface for CO_2 have $2\nu_3$ in the upper level; therefore, measurement of the intensity is necessary for some of these bands.

The strongest of these bands, $(01^12)_I\leftarrow(00^00)_I$ at 5315.7 cm^{-1}, was readily measureable in two spectra that we obtained at the Kitt Peak solar Fourier Transform Spectrometer in 1993. Giver *et al.* [8] reported a preliminary measurement of the intensity of this band; the 1996 HITRAN [9] value for this band, which is based on this preliminary measurement, is also presented in Table 1. The most recent version of HITRAN described by Rothman *et al.* [10], released in December, 2000, has no changes for CO_2 from the prior 1996 version.

In the future, measured intensities of some of these bands could be included in DND calculations described by Wattson and Rothman [5] to improve the dipole-moment surface, and thereby improve the calculated values of higher overtone-combination bands, especially the $(21^12)_{II}\leftarrow(00^00)_I$ band at 7901 cm^{-1} and other nearby bands that are significant in Venus near-infrared emission windows. We therefore decided to obtain spectra at several more path length and pressure conditions in order to measure the

$(01^12)_I \leftarrow (00^00)_I$ band at 5315.7 cm^{-1} as accurately as possible. This article reports our final intensity measurements from these spectra for the $(01^12)_I \leftarrow (00^00)_I$ band at 5315.7 cm^{-1} and the three related nearby perpendicular hot bands listed in Table 1.

These four bands are similar to the ν_2 fundamental and the 3 nearby hot bands arising from the ν_2 level. The intensity of these bands, $(01^10)_I \leftarrow (00^00)_I$, $(02^20)_I \leftarrow (01^10)_I$, $(10^00)_I \leftarrow (01^10)_I$, and $(10^00)_{II} \leftarrow (01^10)_I$ have been measured very well by Johns and Vander Auwera [11]. The four bands in the 5300 cm^{-1} region have similar vibrational assignments, with $2\nu_3$ added to the upper level of each band.

An additional unrelated hot band, $(30^01)_I \leftarrow (10^00)_{II}$ appears in this spectral region at 5217.7 cm^{-1}. This is one of the 8 hot bands arising from the $(10^00)_I$ and $(10^00)_{II}$ levels associated with the $(20^01) \leftarrow (00^00)$ triad parallel bands near 5000 cm^{-1}. Since some of its lines overlapped the region of the 5248 cm^{-1} band, we included it in this study.

EXPERIMENTAL DETAILS

The first two spectra of CO_2 covering the 3800 to 8400 cm^{-1} region were obtained at Kitt Peak, AZ National Solar Observatory with the McMath FTS equipped with a quartz beamsplitter and InSb detectors. An additional 5 spectra of CO_2 and one empty cell spectrum were subsequently obtained with the same apparatus; all spectra had resolution of 0.0102 cm^{-1}. One more spectrum with resolution of 0.0116 cm^{-1} was obtained using a CaF_2 beamsplitter; this spectrum at the lowest pressure was only used for line position measurements. All these spectra utilized a 6-meter base path White cell [12] and research grade CO_2, which had a stated minimum purity of 99.995%. The CO_2 pressures were measured with a 100-Torr MKS Baratron manometer with digitized readout. In addition, a 2.4-m single-pass cell was placed in series with the White cell for low pressure CO 2-0 band line position calibration and instrument lineshape determination. The experimental conditions of all 9 spectra are given in Table 2. The Kitt

Peak interferograms were obtained with 1.3 hours integration time and transformed with the weak "Brault" apodization (discussed by Spencer *et al.*, [13]).

The region of the Q branch of the $(01^12)_I \leftarrow (00^00)_I$ band is shown in Figure 1, and similarly the region of the Q branch of the strongest hot band, $(02^22)_I \leftarrow (01^10)_I$, is shown in Figure 2. As seen in these figures, there are some substantial water vapor lines in this spectral region formed in the air path between the White cell and the FTS despite purging with dry N_2. These lines had to be included in the fitting procedure. For the set of spectra which included an empty cell spectrum, the water lines could be fitted directly on the empty cell spectrum; those fits were then applied to the CO_2 spectra since the water spectrum remained consistent for the entire set and was independent of the White cell path length and CO_2 pressure. Surprisingly, only a few CO_2 lines could not be measured because of the severe water vapor contamination.

Following the procedures described in Giver *et al.* [3], CO_2 line intensities were determined using non-linear least-squares fitting of the spectra. Line profiles were computed using the laboratory conditions for each spectrum, the instrumental profile, and the self-broadening coefficient for each line as given in 1992 HITRAN [4]. However, before accepting these broadening coefficients, we fit the self-broadening coefficients along with the intensities for 15 of the more isolated lines using the spectrum obtained with 80 torr, our highest pressure. These measured broadening coefficients on the 80 torr spectrum averaged only 2% higher than the Rothman *et al.* [4] 1992 HITRAN values, with a standard deviation of ±2%. These measurements on the 5315 cm^{-1} band are not significantly different from the 1992 HITRAN values, which were averaged from measurements on 3 other bands, and therefore our measurements support the 1992 revision of the 1986 HITRAN [7] CO_2 self-broadening coefficients.

The lines of these CO_2 bands were then fitted individually wherever possible on all the spectra, holding the parameters of all nearby lines fixed at their approximate values. During the fit of each spectral line, the position and intensity were adjusted for the calculated spectrum until the sum of the squares of the differences between the observed and calculated line profiles was minimized. The intensities were measured in units of $cm^{-1}/(molecule/cm^2)$ at the temperature of each spectrum, using the total measured pressure without correction for isotopic abundance. These line intensities for each spectrum were then standardized to T = 296 K so the measurements from different spectra could be averaged. The averaged line intensities, S_{obs}, are listed in Tables 3 through 7 for each of the bands, and presented in Figure 3 for the $(01^12)_I \leftarrow (00^00)$ ground-state band. These values are consistent with the HITRAN definition for intensities in a gas with a standard mixture of its isotopomers. Line intensities appropriate for a gas of the pure $^{12}C^{16}O_2$ isotopomer can be obtained by dividing these tabulated values of S_{obs} by the isotopic fraction, f=0.9842.

LINE POSITIONS

The CO_2 line positions determined from the individual fits were then calibrated on each spectrum using the CO 2-0 band [14]. However, these calibrated position measurements cannot be simply averaged for each line, since the spectra were obtained with different pressures. The small pressure shifts should be taken into account so that the line positions at zero pressure can be determined as accurately as possible. This was done for the best determined lines of the ground state band; a linear fit was performed for the calibrated measurements of each line to determine the zero-pressure line position and the pressure shift coefficient. For these lines the pressure shifts were in the range of -0.004 to -0.009 cm^{-1}/atm. This represents a maximum shift of ~0.001 cm^{-1} in our measured positions for the 80 Torr spectrum. Because there is considerable scatter, we

have elected not to report the empirical shifts. However, we note that the magnitude of these shifts is more than a factor of two larger than the shifts given in 1996 HITRAN [9] for the $(00^01)_I \leftarrow (00^00)_I$ fundamental band at 2348 cm^{-1}. This is in agreement with the expectation that pressure shift values increase linearly with increasing wavenumber.

For the lines of the $(01^12)_I \leftarrow (00^00)_I$ band with insufficient measurements for this procedure, an estimated pressure shift, based on results from nearby lines, was applied to the calibrated position measurements. The zero-pressure line positions for this band are listed in Table 3 to 0.0001 cm^{-1}; in all cases these positions agree with 1996 HITRAN [9] positions within the 0.001 cm^{-1} HITRAN maximum uncertainty estimate for these lines. They are similarly close to the measured positions of Arcas *et al.* [15].

The lines of the hot bands, as seen in Figures 1 and 2, are much weaker and therefore the position measurements had less precision. For these lines it was necessary to apply estimated pressure shifts to the average of the calibrated measured positions to determine the zero-pressure line positions; the correction was at most 0.0007 cm^{-1}. Because the line position measurements for the hot bands have more uncertainty than the measurements for the stronger ground-state band, the zero-pressure positions are given in Tables 4 through 7 to only 0.0001 cm^{-1}. For Tables 4, 5 and 7, the positions agree with the HITRAN values within the combined HITRAN uncertainties and our tabulated uncertainties for almost all lines. The weakest band we measured, $(10^02)_I \leftarrow (01^10)_I$, does not appear on the 1992 and 1996 HITRAN tabulations [4, 9], because it was presumed to be too weak for the HITRAN intensity cutoff, although it was on the 1986 version of HITRAN [7].

DETERMINATION OF BAND INTENSITY PARAMETERS

The rotationless transition moment squared and Herman-Wallis intensity parameters for each band were obtained from the measured line intensities standardized to T = 296 K via the theoretical expression for the individual line intensities,

$$S_{J''} = \{8\pi^3 10^{-36}/[3hcg_v Q_{vr}(T)]\}\{\nu f \exp(-E''hc/kT)\}L(J'',\ell)|R_v|^2F(m), \quad (1)$$

where the line intensity is in units of $cm^{-1}/(molecule/cm^2)$, the rovibrational partition function from Gray and Young [16] for $^{12}C^{16}O_2$ is $Q_{vr}(296\ K)=286.14$, the square of the rotationless transition moment $|R_v|^2$ has units of $Debye^2$, J" is the lower state rotational quantum number, and f=0.9842 is the isotopic fraction for $^{12}C^{16}O_2$. The lower state rotational energy levels E"(cm^{-1}) were adopted from the HITRAN tabulations [9], and the line positions $\nu(cm^{-1})$ were determined from our spectral fitting procedures. T is the Kelvin temperature and k, h and c have their usual definitions. The degeneracy factor $g_v=2$ for bands when both the upper and lower states have non-zero vibrational angular momentum ($\ell>0$), since all rotational levels are permitted. This is the case for the $(02^20)_I \leftarrow (01^10)_I$ band at 5291 cm^{-1}; for the other bands $g_v=1$. The Hönl-London linestrength factors $L(J'',\ell)$ for perpendicular bands and the Herman-Wallis factors F(m) were adopted from Rothman *et al.* [4], where m = -J", J", and J"+1 in the P, Q, and R branches respectively.

Solving Eq. 1 for $|R_v|^2F(m)$, we defined the reduced line intensity as $|R_v|^2F(m) = S_{red}(m)$,

$$|R_v|^2F(m) = \{3hc10^{36}/8\pi^3\nu f L(J'',\ell)\}\{S_{J''}g_v Q_{vr}(T)\exp(E''hc/kT)\}. \quad (2)$$

The Herman-Wallis factor is

$$F(m) = [1 + A_1 m + A_2 m^2 + A_3 m^3]^2 \quad (3)$$

for the P and R branches, and

$$F(m) = [1 + B_2 m^2]^2 \qquad (4)$$

for the Q branch. To determine the band intensity parameters, we performed weighted nonlinear least-squares fits for each band to the square root of the experimentally determined reduced intensities:

$$|R_v|[1 + A_1 m + A_2 m^2 + A_3 m^3] = [S_{red}(m)]^{1/2} \qquad (5)$$

for the P and R branches, and

$$|R_v|[1 + B_2 m^2] = [S_{red}(m)]^{1/2} \qquad (6)$$

for the Q branch. Eq. 5 and Eq. 6 were fitted simultaneously to obtain a single value of $|R_v|$ from all the branches of each band. In this work the cubic coefficient A_3 could not be determined for any of the 5 bands.

We followed the suggestion of Devi *et al.* [17], and assigned a weight for each line in Tables 3 through 7 equal to the number of spectra on which it was measured unless the standard deviation of the measurements was unusually high and exceeded a maximum acceptable value δ (expressed in percent) chosen for each band. For these lines weights were calculated as the square of the ratio of δ divided by the standard deviation of the mean listed in Tables 3 through 7.

The simultaneous fits of the line intensities for the P and R branches to Eq. 5 and for the Q branch to Eq. 6 returned values and standard errors for $|R_v|$ and some of the Herman-Wallis parameters for each band. Figure 4 shows the result of fitting the square root of our reduced experimental intensities *vs* m for the P and R branches of the ground-state $(01^12)_I \leftarrow (00^00)_I$ band while the Q branch was fit simultaneously to Eq. 6. This figure shows a quadratic fit, utilizing the A_1 and A_2 Herman-Wallis fitting parameters. Since a cubic fit was not an improvement over this quadratic fit, the A_3 parameter could not be determined. The error bars are $(\Delta S\%/100)[S_{red}(m)]^{1/2}$, where the $\Delta S\%$ are half the values listed in column 6 of Tables 3. Figure 5 shows the result of the

simultaneous fit for the Q branch of this band, plotting the square root of our reduced experimental intensities vs. J^2; the B_2 Herman-Wallis parameter is proportional to the slope of the linear fit. The parameters $|R_v|$, A_1, A_2, $B_{2,\text{ and}}$ $|R_v|^2$ obtained from these fits for the $(01^12)_I \leftarrow (00^00)_I$ band are presented in Table 8. The accompanying uncertainties are 2σ standard deviations of the mean; their determinations have been discussed by Giver *et al.* [3]. The parameters for the 4 hot bands determined in our fits are presented in Tables 8 and 9. The A_2 parameter could only be determined for the $(30^01)_I \leftarrow (10^00)_{II}$ parallel hot band, and the B_2 parameters have substantial uncertainties.

The rotationless band strengths, S^o_v as used in the 1992 HITRAN [4] tabulation, were evaluated at 296 K from these values of the rotationless transition moment:

$$S^0_v(T) = \{8\pi^3 10^{-36}/[3hcQ_v(T)]\}\nu_o f \{\exp(-G''_v hc/kT)\}|R_v|^2 \qquad (7)$$

using the value [16] of the vibrational partition function $Q_v(296\text{ K})=1.0846$; ν_o is the band origin, and G''_v is the lower vibrational energy level. The $S^o_v(296\text{ K})$ results are included in Table 8 and 9.

The total band strengths, S_{Band}, are also reported in Tables 8 and 9; these were obtained by summing the calculated line intensities over each entire band. S_{Band} is nearly equal to S^o_v for the $(02^22)_I \leftarrow (01^10)_I$ band, since its Herman-Wallis parameters are very small. Negative values of A_2 and B_2 cause S_{Band} to be slightly smaller than S^o_v for the $(01^12)_I \leftarrow (00^00)$ band.

CONCLUSIONS

The primary goal of this work was to measure the intensity of the $(01^12)_I \leftarrow (00^00)$ as accurately as possible. As shown in Table 8, the 2σ uncertainties for $|R_v|^2$, S^o_v, and S_{Band} are slightly under 1%. The uncertainty for the Herman-Wallis A_1 parameter is only 2%, the A_2 parameter about 10%, and the B_2 parameter about 15%.

Comparing our final S^{o}_{v} measurement in Table 8 with the HITRAN values in Table 1, we note that the current (1996) HITRAN value is only about 1.7% higher than our final measurement given in Table 8. This HITRAN value was based on the preliminary measurements [8] of the first 2 spectra listed in Table 2.

Our final result for S^{o}_{v} exceeds the older HITRAN values; it is about 20% larger than the 1986 HITRAN value [7] and nearly 3 times larger than the 1992 HITRAN value [4]. The 1986 HITRAN tabulation has no Herman-Wallis parameters for this band. The 1992 HITRAN table has values for the A_1 and A_2 parameters, but not B_2; however, they differ substantially from our measured values. The 1992 table from Rothman *et al.* [4] lists A_1=0.00315, and A_2=0.268x10^{-5}. Their A_1 value is nearly twice our measured value, while their A_2 value has the opposite sign and a much smaller absolute value.

Comparisons for the $(02^{2}2)_{I}\leftarrow(01^{1}0)_{I}$ band, the strongest hot band, is quite similar. Our measured S^{o}_{v} exceeds the 1986 HITRAN value by about 30%, and the 1992 HITRAN value by about a factor of 3. Again, the Herman-Wallis parameters in 1992 HITRAN have no correspondence to our measured values. Our measurements of the weaker $(10^{0}2)_{II}\leftarrow(01^{1}0)_{I}$ band are also stronger than the HITRAN values: our S^{o}_{v} is 35% stronger than the 1986 HITRAN, and about 60% stronger than the 1992 HITRAN. For the weakest $(10^{0}2)_{I}\leftarrow(01^{1}0)_{I}$ band, our measured S^{o}_{v} is only 1% higher than Rothman's [7] 1986 HITRAN value; the values fortuitously agree within our 5% 2σ uncertainty. Because of the HITRAN intensity cutoff, this band was omitted from the 1992 HITRAN tabulations; the more recent versions of HITRAN are unchanged from the 1992 version for all 4 hot bands we measured.

Our measured S^{o}_{v} intensity for the $(30^{0}1)_{I}\leftarrow(10^{0}0)_{II}$ parallel hot band is only slightly stronger than the HITRAN values, although our 2σ uncertainty is only 1.4%. Our value exceeds the 1986 HITRAN value adopted from the DND computations of

Wattson and Rothman [18] by 3.6%, and the 1992 HITRAN value by nearly 10%. Again, the older HITRAN has no Herman-Wallis parameters to compare to our measured values. The small A_1 parameter in the 1992 HITRAN tabulation has the opposite sign, although the same absolute value, as our measured value. Their value of A_2=-4.11x10^{-5} agrees with our measured value within our 2σ uncertainty.

Johns and Auwera [11] have determined $|R_v|^2$ values for bands in the ν_2 fundamental region. The four strongest bands in that region, $(01^10)_I \leftarrow (00^00)_I$, $(02^20)_I \leftarrow (01^10)_I$, $(10^00)_{II} \leftarrow (01^10)_I$, and $(10^00)_I \leftarrow (01^10)_I$, differ from the four perpendicular bands we are reporting here only in that there is no excitation in the ν_3 vibration. The ratio of the sum of the $|R_v|^2$ values for the 3 hot bands to the ground state band $|R_v|^2$ value is relatively unchanged in going to the higher vibrational excitation, and indicates only a small effect of mechanical and electrical anharmonicity on the intensity of the bands we have measured, Fermi resonance not withstanding. For the ν_2 fundamental region the ratio for the sum of the three ℓ = 0, 2 hot bands to the ν_2 fundamental band is 2.93; for the bands reported here that ratio is equal to 2.96. These ratios are equivalent within the experimental uncertainties.

ACKNOWLEDGEMENTS

We wish to thank Claude Plymate of KPNO for all his help operating the Kitt Peak McMath FTS and White Cell, and obtaining some of these spectra. We also appreciate the collaboration of Richard Wattson; he provided us his DND calculated line lists, and was always eager to compare results of our measurements with his calculated values. We regret his passing on Feburary 23, 2000.

Part of the research described in this paper was performed at the Jet Propulsion Laboratory, California Institute of Technology, under contract with The National Aeronautics and Space Administration.

REFERENCES

1. Pollack JB, Dalton JB, Grinspoon D, Wattson RB, Freedman R, Crisp D, Allen DA, Bezard B, DeBergh C, Giver LP, Ma Q, Tipping R. Near-infrared light from Venus' nightside: a spectroscopic analysis. *Icarus* 1993;**103**:1-42.

2. Giver LP, Chackerian Jr. C. Rovibrational intensities for the $(31^10)_{IV}$-(00^00) band of $^{12}C^{16}O_2$ at 4416 cm^{-1}. *J Molec Spectrosc* 1991;**148**:80-85.

3. Giver LP, Chackerian Jr. C, Spencer MN, Brown LR, Wattson RB. The rovibrational intensities of the (4001)-(0000) pentad absorption bands of $^{12}C^{16}O_2$ between 7284 and 7921 cm^{-1}. *J Molec Spectrosc* 1996;**175**:104-111.

4. Rothman LS, Hawkins RL, Wattson RB, Gamache RR. Energy levels, intensities, and linewidths of atmospheric carbon dioxide bands. *J Quant Spectrosc Radiat Transfer* 1992;**48**:537-566.

5. Wattson RB, Rothman LS. Direct numerical diagonalization: wave of the future. *J Quant Spectrosc Radiat Transfer* 1992;**48**:763-780.

6. McClatchey EA, Benedict WS, Clough SA, Burch DE, Calfee RF, Fox K, Rothman LS, Garing JS. "AFCRL atmospheric absorption line parameters compilation," AFCRL TR-73-0096 (AFCRL, Bedford, MA, 1973), AD #762904.

7. Rothman LS. Infrared energy levels and intensities of carbon dioxide. *Appl Opt* 1986;**25**:1795-1816.

8. Giver LP, Chackerian Jr. C, Spencer MN, Freedman RS, Brown LR, Wattson RB. Intensity and self-broadening measurements of the 01^121-00^001 CO_2 perpendicular band at 5315 cm^{-1}. Seventh International Conference on Laboratory Research for Planetary Atmospheres, Kona, HI (Oct. 8, 1995).

9. Rothman LS, Rinsland CP, Goldman A, Massie ST, Edwards DP, Flaud J-M, Perrin A, Camy-Peyret C, Dana V, Mandin J-Y, Schroeder J, McCann A, Gamache RB, Wattson RB, Yoshino K, Chance KV, Jucks KW, Brown LR, Nemtchinov V, Varanasi P. The HITRAN molecular spectroscopic database and HAWKS: 1996 edition *J Quant Spectrosc Radiat Transfer* 1998;**60**:665-710.

10. Rothman LS, Chance K, Schroeder J, Goldman A. New edition of HITRAN database. Proceedings of the Eleventh Atmospheric Radiation Measurement (ARM) Science Team Meeting, Atlanta, GA (March, 2001).

11. Johns JWC, Vander Auwera J. Absolute intensities in CO_2: the ν_2 fundamental near 15 μm. *J Molec Spectrosc* 1990;**140**:71-102.

12. White JU. Long optical paths of large aperture. *J Opt Soc Am* 1942;**32**;285-288.

13. Spencer MN, Chackerian Jr. C, Giver LP, Brown LR. The nitric oxide fundamental band: frequency and shape parameters for rovibrational lines. *J Molec Spectrosc* 1994;**165**:506-524.

14. Pollock CR, Petersen FR, Jennings DA, Wells JS. Absolute frequency measurement of the 2-0 band of CO at 2.3μm; Calibration standard frequencies from high resolution color center laser spectroscopy. *J Molec Spectrosc* 1983;**99**:357-368.

15. Arcas P, Arie E, Cuisenier M, Maillard JP. The infrared spectrum and molecular constants of CO_2 in the 2 μm region. *Can J Phys* 1983;**61**:857-866.

16. Gray LD, Young AT. Relative intensity calculations for carbon dioxide - IV: Calculations of the partition function for isotopes of CO_2. *J Quant Spectrosc Radiat Transfer* 1969;**9**:569-589.

17. Devi VM, Rinsland CP, Benner DC. Absolute intensity measurements of CO_2 bands in the 2395 - 2680 cm^{-1} region. *Appl Opt* 1984;**23**:4067-4075.

18. Wattson RB, Rothman LS. Determination of vibrational energy levels and parallel band intensities of $^{12}C^{16}O_2$ by direct numerical diagonalization. *J Molec Spectrosc* 1986;**119**:83-100.

Table 1. Positions and Intensities of the $(n1^12)\leftarrow(00^00)$ bands and hot bands.

Band	Band Origin (cm^{-1})	1986 Hitran Intensity[a]	1992 Hitran Intensity[b]	1996 Hitran Intensity[c]
$(00^02)_I\leftarrow(01^10)_I$	4005.946	0.00818	0.0385	0.00818
$(10^02)_{II}\leftarrow(01^10)_I$	5247.832	0.0101	0.00846	0.00846
$(02^22)_I\leftarrow(01^10)_I$	5291.132	0.0275	0.0121	0.0121
$(01^12)_I\leftarrow(00^00)_I$	5315.713	0.398	0.168	0.484
$(10^02)_I\leftarrow(01^10)_I$	5349.310	0.00506	-.----	-.----
$(11^12)_{II}\leftarrow(00^00)_I$	6537.959	0.0223	0.00598	0.0186
$(11^12)_I\leftarrow(00^00)_I$	6679.706	0.0283	0.0148	0.0285
$(21^12)_{III}\leftarrow(00^00)_I$	7743.673	0.0004	-.----	-.----
$(21^12)_{II}\leftarrow(00^00)_I$	7901.479	0.00149	0.00149	0.00149
$(21^12)_I\leftarrow(00^00)_I$	8055.939	-.----	-.----	-.----
$(30^01)_I\leftarrow(10^00)_{II}$	5217.673	0.0220	0.0208	0.0208

[a] S^0_v Intensities in units of 10^{-22} $cm^{-1}/(molecule/cm^2)$ at 296 K; from Ref. (7).

[b] S^0_v Intensities from Ref. (4).

[c] S^0_v Intensities from Ref. (9).

Table 2. Experimental Conditions of the Kitt Peak McMath FTS CO_2 Spectra.

Spectrum Number	Path Length (m)	Pressure (torr)	Temperature (K)	Resolution cm^{-1}
1	73.0	59.7	297.8	0.0102
2	193.3	59.7	298.0	0.0102
3	48.9	0.0	297.3	0.0102
4	48.9	80.0	297.4	0.0102
5	97.0	65.0	297.6	0.0102
6	409.8	45.0	297.8	0.0102
7	145.2	45.0	297.8	0.0102
8	24.9	30.0	297.0	0.0102
9	313.6	21.5	296.5	0.0116

Table 3. Line positions and intensities for the $(01^12)_I \leftarrow (00^00)$ band of $^{12}C^{16}O_2$.

Line	$\nu(cm^{-1})^a$	n[b]	wt[c]	S_{obs}[d]	$2\Delta S\%$[e]	S_{cal}[d]	$(S_{obs}-S_{cal})/S_{cal}\%$
P 52	5260.15812(74)	3	0.13	0.190	8.3	0.185	2.9
P 50	5262.85795(48)	3	0.15	0.281	7.8	0.267	5.3
P 48	5265.51234(57)	2	2.00	0.375	1.0	0.377	-0.2
P 46	5268.12161(38)	6	2.04	0.532	2.1	0.525	1.3
P 44	5270.68580(13)	6	1.20	0.732	2.7	0.719	1.8
P 42	5273.20626(27)	6	5.62	0.975	1.3	0.967	0.8
P 40	5275.68008(23)	6	4.62	1.319	1.4	1.277	3.3
P 38	5278.11030(9)	6	6.00	1.652	0.4	1.656	-0.3
P 36	5280.49524(12)	6	6.00	2.108	0.9	2.109	-0.03
P 34	5282.83527(22)	7	2.98	2.639	1.7	2.635	0.14
P 32	5285.12999(19)	7	1.99	3.22	2.1	3.23	-0.3
P 30	5287.38000(16)	6	6.00	3.85	0.7	3.88	-0.8
P 26	5291.74469(12)	6	6.00	5.15	0.6	5.28	-2.5
P 24	5293.85916(10)	7	7.00	5.87	0.9	5.96	-1.4
P 22	5295.92883(10)	7	7.00	6.48	0.7	6.57	-1.4
P 20	5297.95359(7)	7	7.00	6.99	0.6	7.08	-1.2
P 18	5299.93278(11)	6	5.08	7.42	1.3	7.41	0.1
P 16	5301.86735(8)	5	5.00	7.51	0.4	7.54	-0.4
P 14	5303.75650(9)	6	6.00	7.37	1.0	7.42	-0.7
P 12	5305.60031(8)	6	6.00	7.06	0.7	7.03	0.4
P 8	5309.15242(11)	7	7.00	5.34	0.7	5.34	0.0
P 6	5310.86059(17)	7	7.00	4.04	0.8	4.07	-0.7
P 4	5312.52372(24)	7	7.00	2.695	0.8	2.56	5.0
P 2	5314.14208(30)	2	0.10	0.824	9.5	0.886	-7.0
Q 60	5297.05420(75)	2	0.03	0.099	19.0	0.098	0.6
Q 58	5298.26878(72)	4	0.10	0.169	9.6	0.151	12.2
Q 56	5299.44351(28)	4	0.43	0.230	4.8	0.226	1.7
Q 54	5300.57645(45)	6	0.30	0.329	5.4	0.334	-1.4
Q 52	5301.66843(45)	6	0.70	0.492	3.8	0.483	0.9
Q 48	5303.72875(21)	6	0.56	1.015	4.0	0.968	4.8
Q 46	5304.69831(14)	6	2.16	1.350	2.0	1.335	1.1
Q 44	5305.62646(10)	6	6.00	1.820	0.7	1.811	0.5
Q 42	5306.51302(12)	6	6.00	2.435	1.2	2.413	0.9
Q 38	5308.16477(10)	6	6.00	4.04	0.8	4.07	-0.7
Q 36	5308.92909(13)	7	6.23	5.09	1.2	5.14	-0.9
Q 34	5309.65281(9)	7	7.00	6.35	0.8	6.37	-0.3
Q 32	5310.33561(11)	6	6.00	7.68	0.5	7.76	-1.1
Q 30	5310.97744(10)	6	6.00	9.16	0.6	9.27	-1.2
Q 28	5311.57852(9)	6	6.00	10.80	0.7	10.86	-0.6
Q 26	5312.13891(11)	6	6.00	12.40	0.6	12.46	-0.5
Q 24	5312.65828(9)	6	6.00	13.94	0.4	14.01	-0.5
Q 22	5313.13700(8)	5	5.00	15.39	0.7	15.41	-0.1
Q 20	5313.57494(8)	5	5.00	16.55	0.6	16.55	0.0
Q 18	5313.97206(9)	5	5.00	17.30	0.6	17.35	-0.3
Q 16	5314.32847(9)	5	5.00	17.72	0.5	17.69	0.2
Q 14	5314.64420(7)	5	5.00	17.51	0.8	17.51	0.0
Q 12	5314.91907(8)	5	5.00	16.79	0.7	16.75	0.3
Q 10	5315.15341(13)	5	5.00	15.59	0.5	15.36	1.5
Q 8	5315.34677(7)	6	6.00	13.48	0.6	13.37	0.8
Q 6	5315.49948(6)	6	6.00	10.86	0.6	10.83	0.3
Q 4	5315.61132(16)	7	5.72	7.86	1.2	7.82	0.5
Q 2	5315.68252(23)	7	7.00	4.42	1.0	4.47	-1.1

R 0	5316.48339(42)	5	1.55	1.900	2.4	1.813	4.8
R 2	5317.98654(22)	6	6.00	3.634	0.9	3.612	0.6
R 4	5319.44517(19)	7	7.00	5.31	0.7	5.32	-0.1
R 6	5320.85864(11)	7	7.00	6.87	0.8	6.84	0.4
R 8	5322.22653(12)	6	6.00	8.16	0.7	8.13	0.4
R 10	5323.54867(11)	6	6.00	9.28	0.5	9.14	1.6
R 12	5324.82565(9)	6	6.00	9.88	0.3	9.83	0.5
R 14	5326.05697(8)	5	5.00	10.22	0.6	10.22	0.0
R 18	5328.38277(8)	6	6.00	10.07	0.5	10.07	0.0
R 20	5329.47716(10)	6	6.00	9.63	0.6	9.60	0.3
R 22	5330.52618(9)	6	6.00	8.92	0.5	8.95	-0.4
R 24	5331.52933(11)	6	6.00	8.14	0.4	8.17	-0.3
R 26	5332.48667(10)	6	6.00	7.21	0.7	7.23	-0.3
R 28	5333.39823(11)	7	7.00	6.27	0.7	6.32	-0.8
R 30	5334.26408(12)	7	7.00	5.38	0.6	5.40	-0.4
R 32	5335.08424(11)	7	6.08	4.544	1.2	4.541	0.1
R 34	5335.85873(16)	6	6.00	3.726	0.6	3.743	-0.4
R 36	5336.58654(12)	7	7.00	2.997	0.8	3.028	-1.0
R 38	5337.26937(10)	7	3.86	2.388	1.5	2.405	-0.7
R 40	5337.90576(11)	7	3.20	1.885	1.7	1.878	0.4
R 42	5338.49632(49)	3	1.10	1.535	2.9	1.441	6.5
R 44	5339.04010(91)	5	0.38	1.105	4.8	1.085	1.8
R 46	5339.53932(21)	6	1.04	0.788	2.9	0.804	-2.0
R 50	5340.39818(59)	5	0.44	0.432	4.5	0.419	3.0
R 52	5340.75842(38)	2	0.10	0.302	9.3	0.295	2.3
R 54	5341.07229(40)	2	0.17	0.195	7.3	0.204	-4.5
R 56	5341.34023(58)	2	0.31	0.147	5.4	0.140	5.2

[a]Measured line positions adjusted to zero pressure.

[b]Number of measurements.

[c]Weight used in least-squares fit for intensity parameters.

[d]Line intensity in units of 10^{-25} $cm^{-1}/(molecule/cm^2)$ at 296 K. Intensities appropriate for a gas of the pure $^{12}C^{16}O_2$ isotopomer can be obtained by dividing these tabulated values of S_{obs} by the isotopic fraction, f=0.9842.

[e]Twice the standard deviation of the mean of S_{obs}, as percentage of S_{obs}.

Table 4. Line positions and intensities for the $(10^02)_{II}\leftarrow(01^10)_I$ band of $^{12}C^{16}O_2$.

Line	$\nu(cm^{-1})^a$	n[b]	wt[c]	S_{obs}[d]	$2\Delta S\%$[e]	S_{cal}[d]	$(S_{obs}-S_{cal})/S_{cal}\%$
P 23	5226.7723 (22)	2	2.00	0.106	11.6	0.096	10.3
P 21	5228.8614 (21)	4	1.78	0.130	15.1	0.114	13.6
P 17	5232.8904 (21)	4	4.00	0.150	4.8	0.147	1.8
P 15	5234.8306 (10)	5	5.00	0.151	9.0	0.160	-6.0
P 13	5236.7239 (24)	1	0.66	0.159		0.168	-5.7
P 9	5240.3618 (11)	4	2.44	0.152	12.8	0.164	-7.8
P 7	5242.1063 (11)	3	2.02	0.135	14.1	0.150	-10.2
P 3	5245.4509 (36)	1	0.39	0.090		0.092	-2.5
Q 40	5236.7478 (24)	1	0.38	0.0828		0.0833	-0.6
Q 38	5237.8185 (15)	2	1.34	0.101	17.3	0.108	-6.2
Q 36	5238.8376 (3)	3	2.72	0.144	11.9	0.138	4.4
Q 34	5239.7993 (5)	5	3.05	0.168	11.4	0.172	-2.3
Q 30	5241.5591 (7)	4	4.00	0.253	5.5	0.253	-0.2
Q 28	5242.3567 (11)	5	5.00	0.302	5.1	0.299	1.2
Q 26	5243.1011 (3)	5	5.00	0.333	1.8	0.345	-3.4
Q 20	5245.0039 (5)	6	6.00	0.466	2.5	0.464	0.3
Q 18	5245.5302 (5)	6	6.00	0.485	4.4	0.488	-0.7
Q 16	5246.0009 (3)	6	6.00	0.528	3.8	0.500	5.6
Q 14	5246.4191 (3)	6	6.00	0.511	4.9	0.496	3.1
Q 12	5246.7829 (3)	6	6.00	0.477	3.9	0.475	0.2
Q 10	5247.0918 (8)	6	6.00	0.443	4.3	0.437	1.4
Q 4	5247.6980 (3)	2	0.71	0.240	23.8	0.224	7.3
R 5	5252.2622 (16)	2	2.00	0.141		0.144	-2.0
R 7	5253.6416 (16)	3	3.00	0.203	5.8	0.203	0.1
R 11	5256.2533 (4)	5	5.00	0.306	5.1	0.305	0.2
R 13	5257.4844 (10)	5	5.00	0.344	3.5	0.344	-0.1
R 15	5258.6659 (26)	1	1.00	0.372		0.373	-0.4
R 17	5259.7993 (12)	5	5.00	0.387	3.2	0.391	-1.0
R 19	5260.8830 (5)	5	5.00	0.397	4.0	0.397	-0.2
R 21	5261.9171 (8)	4	4.00	0.372	1.0	0.393	-5.4
R 23	5262.9016 (3)	5	5.00	0.409	2.7	0.379	8.0
R 27	5264.7206 (5)	5	5.00	0.305	3.5	0.329	-7.4
R 29	5265.5554 (7)	4	1.98	0.263	14.2	0.296	-11.2
R 31	5266.3379 (5)	5	5.00	0.263	2.5	0.262	0.6
R 33	5267.0727 (5)	5	5.00	0.223	4.0	0.226	-1.4
R 35	5267.7546 (15)	3	3.00	0.190	9.7	0.192	-1.2
R 37	5268.3877 (10)	3	2.64	0.186	12.3	0.160	16.6

[a]Average measured line positions with twice the standard deviation of the mean uncertainty.

[b]Number of measurements.

[c]Weight used in least-squares fit for intensity parameters.

[d]Line intensity in units of 10^{-25} $cm^{-1}/(molecule/cm^2)$ at 296 K. Intensities appropriate for a gas of the pure $^{12}C^{16}O_2$ isotopomer can be obtained by dividing these tabulated values of S_{obs} by the isotopic fraction, f=0.98442.

[e]Twice the standard deviation of the mean of S_{obs}, as percentage of S_{obs}.

Table 5. Line positions and intensities for the $(02^{2}2)_{I} \leftarrow (01^{1}0)_{I}$ band of $^{12}C^{16}O_2$.

Line	$\nu(cm^{-1})^a$	n^b	wt^c	$S_{obs}{}^d$	$2\Delta S\%^e$	$S_{cal}{}^d$	$(S_{obs}-S_{cal})/S_{cal}\%$
P 35	5257.8229 (12)	2	2.00	0.096	9.9	0.096	0.0
P 34	5258.2118 (9)	2	0.96	0.116	14.3	0.106	9.3
P 33	5260.0572 (10)	3	0.63	0.130	17.6	0.117	11.2
P 32	5260.5059 (15)	3	0.81	0.132	15.6	0.128	3.0
P 31	5262.2491 (23)	2	2.00	0.150	9.9	0.140	7.1
P 30	5262.7573 (12)	3	3.00	0.148	8.1	0.152	-2.9
P 28	5264.9638 (9)	3	1.84	0.210	10.3	0.177	19.2
P 27	5266.5159 (9)	3	1.59	0.186	11.1	0.189	-1.6
P 26	5267.1264 (11)	3	3.00	0.193	7.6	0.201	-3.8
P 25	5268.5892 (21)	3	3.00	0.199	6.9	0.213	-6.4
P 23	5270.6231 (12)	5	5.00	0.220	6.2	0.234	-5.8
P 22	5271.3130 (9)	5	3.33	0.237	7.7	0.242	-2.4
P 21	5272.6168 (3)	5	3.60	0.243	7.4	0.250	-3.1
P 20	5273.3406 (11)	5	5.00	0.261	5.2	0.256	1.7
P 19	5274.5713 (9)	5	5.00	0.248	4.5	0.261	-5.0
P 18	5275.3225 (4)	5	5.00	0.298	4.5	0.263	13.3
P 17	5276.4849 (10)	5	5.00	0.247	4.5	0.264	-6.4
P 16	5277.2594 (4)	5	4.77	0.257	6.4	0.262	-2.0
P 15	5278.3587 (7)	5	5.00	0.235	5.4	0.258	-8.9
P 14	5279.1518 (5)	5	4.57	0.254	6.5	0.251	1.4
P 12	5280.9983 (18)	3	3.00	0.217	6.9	0.229	-5.3
P 11	5281.9845 (11)	3	3.00	0.225	6.9	0.214	4.9
P 10	5282.8007 (4)	3	3.00	0.197	6.9	0.197	0.3
P 9	5283.7383 (7)	2	2.00	0.190	8.5	0.177	7.6
P 7	5285.4521 (13)	2	0.88	0.123	14.9	0.130	-5.5
P 6	5286.2679 (6)	2	2.00	0.105	9.9	0.104	0.4
Q 39	5283.2786 (33)	2	1.11	0.138	13.3	0.138	0.1
Q 38	5282.7641 (6)	2	0.97	0.157	14.2	0.155	1.4
Q 37	5284.0536 (8)	3	3.00	0.185	6.9	0.176	5.2
Q 36	5283.6114 (19)	2	2.00	0.187	8.5	0.196	-4.5
Q 34	5284.4132 (6)	3	2.57	0.234	8.7	0.243	-3.6
Q 33	5285.4843 (6)	3	3.00	0.281	7.2	0.269	4.3
Q 32	5285.1686 (2)	3	3.00	0.312	5.8	0.295	5.8
Q 31	5286.1389 (5)	5	5.00	0.312	4.5	0.324	-3.7
Q 30	5285.8813 (5)	5	5.00	0.352	5.1	0.352	0.0
Q 29	5286.7532 (2)	3	3.00	0.386	4.6	0.383	0.8
Q 28	5286.5469 (6)	5	5.00	0.408	3.4	0.412	-0.9
Q 27	5287.3274 (2)	5	5.00	0.432	2.8	0.443	-2.5
Q 26	5287.1681 (5)	5	5.00	0.463	3.4	0.472	-2.0
Q 25	5287.8608 (7)	6	6.00	0.488	4.2	0.503	-2.9
Q 24	5287.7446 (2)	6	6.00	0.511	2.4	0.530	-3.5
Q 23	5288.3541 (6)	6	6.00	0.577	3.0	0.558	3.5
Q 22	5288.2748 (2)	5	5.00	0.579	3.8	0.582	-0.5
Q 21	5288.8074 (3)	5	5.00	0.616	2.7	0.605	1.7
Q 20	5288.7607 (1)	6	6.00	0.661	3.5	0.624	5.9
Q 19	5289.2199 (3)	6	6.00	0.646	2.4	0.641	0.7
Q 18	5289.2011 (5)	6	6.00	0.655	3.7	0.653	0.3
Q 15	5289.9247 (5)	2	1.85	0.645	10.3	0.663	-2.7
Q 14	5289.9463 (2)	2	2.00	0.662	4.5	0.656	1.0
Q 11	5290.4685 (12)	2	1.82	0.595	10.4	0.626	-4.9
Q 10	5290.5110 (5)	2	1.10	0.572	13.4	0.592	-3.3
Q 9	5290.6793 (6)	2	2.00	0.544	4.2	0.569	-4.5

Q 8	5290.7261 (7)	2	2.00	0.499	4.2	0.491	1.7
Q 7	5290.8513 (5)	2	2.00	0.423	6.7	0.443	-4.7
Q 6	5290.8946 (5)	2	2.00	0.391	5.7	0.390	0.5
Q 5	5290.9820 (1)	2	2.00	0.329	5.7	0.331	-0.5
Q 4	5291.0200 (19)	2	2.00	0.261	7.1	0.266	-2.0
R 1	5292.6648 (5)	3	1.20	0.201	12.8	0.204	-1.4
R 2	5293.4132 (14)	3	0.92	0.210	14.6	0.225	-6.8
R 3	5294.1563 (8)	4	2.18	0.277	9.5	0.251	10.3
R 4	5294.8760 (6)	5	3.55	0.293	7.4	0.277	5.8
R 5	5295.6088 (6)	5	5.00	0.317	4.5	0.303	4.7
R 6	5296.2941 (9)	5	5.00	0.330	3.6	0.326	1.2
R 7	5297.0205 (5)	4	4.00	0.349	4.0	0.333	5.0
R 8	5297.6667 (8)	5	5.00	0.363	3.6	0.367	-1.1
R 9	5298.3913 (5)	6	4.44	0.385	6.6	0.384	0.3
R 10	5298.9934 (7)	6	6.00	0.407	4.6	0.397	2.5
R 12	5300.2757 (5)	5	3.55	0.414	7.4	0.415	-0.2
R 13	5301.0123 (4)	5	5.00	0.466	2.7	0.420	10.9
R 14	5301.5127 (3)	6	6.00	0.436	3.4	0.422	3.5
R 15	5302.2623 (7)	5	5.00	0.410	3.8	0.421	-2.6
R 17	5303.4718 (4)	6	6.00	0.391	2.9	0.411	-4.8
R 18	5303.8499 (3)	6	6.00	0.406	2.4	0.402	1.0
R 19	5304.6404 (4)	5	5.00	0.408	2.7	0.391	4.2
R 20	5304.9508 (10)	6	6.00	0.379	5.7	0.378	0.1
R 21	5305.7689 (7)	6	6.00	0.354	5.6	0.365	-2.8
R 22	5306.0057 (5)	5	5.00	0.360	3.6	0.349	3.2
R 23	5306.8565 (1)	6	6.00	0.324	3.5	0.332	-2.6
R 24	5307.0160 (8)	5	5.00	0.306	4.1	0.314	-2.7
R 25	5307.9040 (4)	4	4.00	0.285	5.0	0.297	-3.9
R 26	5307.9790 (7)	4	4.00	0.269	5.7	0.278	-3.2
R 29	5309.8761 (5)	4	4.00	0.207	6.0	0.223	-7.6
R 30	5309.7711 (5)	4	4.00	0.202	6.0	0.205	-1.5
R 31	5310.8022 (3)	3	3.00	0.178	7.5	0.188	-5.7
R 32	5310.5977 (4)	3	3.00	0.181	7.4	0.171	6.0
R 33	5311.6859 (6)	2	2.00	0.145	9.9	0.156	-6.9
R 34	5311.3795 (21)	2	0.62	0.143	17.8	0.140	1.8
R 37	5313.3335 (14)	2	2.00	0.114	9.9	0.101	13.0

[a]Average measured line positions with twice the standard deviation of the mean uncertainty.

[b]Number of measurements.

[c]Weight used in least-squares fit for intensity parameters.

[d]Line intensity in units of 10^{-25} $cm^{-1}/(molecule/cm^2)$ at 296 K. Intensities appropriate for a gas of the pure $^{12}C^{16}O_2$ isotopomer can be obtained by dividing these tabulated values of S_{obs} by the isotopic fraction, f=0.9842.

[e]Twice the standard deviation of the mean of S_{obs}, as percentage of S_{obs}.

Table 6. Line positions and intensities for the $(10^02)_I \leftarrow (01^10)_I$ band of $^{12}C^{16}O_2$.

Line	$\nu(cm^{-1})^a$	n^b	wt^c	$S_{obs}{}^d$	$2\Delta S\%^e$	$S_{cal}{}^d$	$(S_{obs}-S_{cal})/S_{cal}\%$
P 31	5318.8906 (11)	5	5.00	0.164	9.4	0.167	-1.8
P 29	5321.2376 (10)	5	5.00	0.180	9.9	0.185	-3.1
P 25	5325.7724 (8)	5	4.49	0.220	11.3	0.214	2.6
P 23	5327.9601 (19)	5	5.00	0.226	8.8	0.223	1.3
P 21	5330.0956 ((7)	4	4.00	0.234	8.1	0.226	3.7
P 17	5334.2095 (10)	5	4.00	0.213	4.1	0.214	-0.5
P 9	5341.7966 (12)	2	2.00	0.134	3.3	0.129	4.1
P 7	5343.5570 (40)	1	0.67	0.114		0.100	14.1
P 3	5346.9271 (22)	2	0.69	0.047	28.8	0.044	5.6
Q 34	5340.6328 (30)	2	2.00	0.080	10.3	0.074	7.8
Q 32	5341.6054 (21)	2	2.00	0.084	13.0	0.090	-6.0
Q 30	5342.5242 (40)	1	0.68	0.120		0.106	12.9
Q 26	5344.1831 (16)	2	2.00	0.145	13.6	0.140	3.6
Q 22	5345.6133 (8)	5	5.00	0.163	7.8	0.171	-4.6
Q 20	5346.2397 (8)	5	5.00	0.177	10.5	0.182	-2.9
Q 18	5346.8101 (34)	1	0.88	0.208		0.190	9.4
Q 14	5347.7749 (8)	5	5.00	0.190	9.8	0.190	0.2
Q 12	5348.1696 (12)	5	5.00	0.171	5.3	0.181	-5.6
Q 10	5348.5051 (40)	1	0.82	0.168		0.165	1.8
Q 6	5349.0050 (40)	1	0.69	0.123		0.116	6.4
Q 4	5349.1638 (24)	2	2.00	0.084	7.5	0.084	1.0

[a]Average measured line positions with twice the standard deviation of the mean uncertainty.

[b]Number of measurements.

[c]Weight used in least-squares fit for intensity parameters.

[d]Line intensity in units of 10^{-25} $cm^{-1}/(molecule/cm^2)$ at 296 K. Intensities appropriate for a gas of the pure $^{12}C^{16}O_2$ isotopomer can be obtained by dividing these tabulated values of S_{obs} by the isotopic fraction, f=0.9842.

[e]Twice the standard deviation of the mean of S_{obs}, as percentage of S_{obs}.

Table 7. Line positions and intensities for the $(30^01)_I \leftarrow (10^00)_{II}$ band of $^{12}C^{16}O_2$.

Line	$\nu(cm^{-1})^a$	n[b]	wt[c]	S_{obs}[d]	$2\Delta S\%$[e]	S_{cal}[d]	$(S_{obs}-S_{cal})/S_{cal}\%$
P 36	5186.5612 (11)	3	1.87	0.202	7.3	0.208	-2.8
P 34	5188.4368 (3)	3	0.93	0.277	10.4	0.262	5.9
P 32	5190.2974 (6)	5	2.46	0.335	6.4	0.323	3.7
P 30	5192.1424 (6)	6	3.77	0.405	5.2	0.391	3.6
P 28	5193.9717 (4)	6	6.00	0.472	3.4	0.463	2.0
P 26	5195.7840 (6)	6	6.00	0.518	3.8	0.538	-3.6
P 22	5199.3576 (10)	6	3.31	0.661	5.5	0.676	-2.2
P 20	5201.1172 (4)	6	6.00	0.737	2.6	0.732	0.7
P 18	5202.8588 (4)	6	6.00	0.759	1.8	0.772	-1.6
P 16	5204.5825 (6)	6	6.00	0.807	4.0	0.791	2.0
P 12	5207.9716 (5)	6	6.00	0.740	1.6	0.751	-1.5
P 10	5209.6379 (6)	5	5.00	0.679	1.7	0.688	-1.3
P 8	5211.2841 (3)	6	6.00	0.606	2.3	0.594	1.9
P 6	5212.9104 (7)	6	6.00	0.487	2.0	0.474	2.7
P 4	5214.5174 (5)	5	5.00	0.334	3.4	0.331	0.9
R 2	5219.9856 (18)	4	1.46	0.236	8.4	0.257	-8.2
R 4	5221.5013 (4)	6	6.00	0.402	3.3	0.417	-3.5
R 6	5222.9987 (5)	6	4.37	0.560	4.8	0.559	0.2
R 8	5224.4757 (6)	5	5.00	0.688	3.9	0.678	1.6
R 10	5225.9319 (4)	6	6.00	0.780	3.5	0.768	1.5
R 12	5227.3698 (4)	6	6.00	0.824	3.3	0.829	-0.7
R 14	5228.7879 (3)	5	5.00	0.849	1.2	0.860	-1.3
R 16	5230.1862 (3)	6	6.00	0.874	1.9	0.862	1.4
R 18	5231.5655 (4)	3	2.09	0.867	6.9	0.838	3.4
R 20	5232.9260 (3)	6	6.00	0.793	2.4	0.794	-0.1
R 22	5234.2685 (3)	6	6.00	0.733	3.4	0.732	0.1
R 24	5235.5927 (5)	6	6.00	0.670	2.2	0.660	1.5
R 26	5236.8986 (5)	6	6.00	0.587	3.4	0.582	0.8
R 28	5238.1871 (6)	4	4.00	0.493	2.8	0.502	-1.7
R 30	5239.4589 (6)	5	4.48	0.416	4.7	0.424	-1.9
R 34	5241.9537 (9)	5	1.61	0.296	7.9	0.285	3.9
R 36	5243.1763 (7)	5	4.10	0.226	5.0	0.226	-0.1
R 40	5245.5806 (13)	3	0.69	0.142	12.0	0.136	4.5
R 42	5246.7594 (18)	2	0.26	0.102	19.6	0.102	0.6

[a]Average measured line positions with twice the standard deviation of the mean uncertainty.

[b]Number of measurements.

[c]Weight used in least-squares fit for intensity parameters.

[d]Line intensity in units of 10^{-25} $cm^{-1}/(molecule/cm^2)$ at 296 K. Intensities appropriate for a gas of the pure $^{12}C^{16}O_2$ isotopomer can be obtained by dividing these tabulated values of S_{obs} by the isotopic fraction, f=0.9842.

[e]Twice the standard deviation of the mean of S_{obs}, as percentage of S_{obs}.

TABLE 8. Intensity Parameters for the 5315 cm^{-1} and 5291 cm^{-1} Bands of $^{12}C^{16}O_2$.

Parameter*	$(01^12)_I \leftarrow (00^00)_I$	$(02^22)_I \leftarrow (01^10)_I$
ν_0	5315.713 cm^{-1}	5291.132 cm^{-1}
$\|R_v\|$	$(15.40 \pm 0.07)\times10^{-5}$ Debye	$(21.48 \pm 0.16)\times10^{-5}$ Debye
A_1	$+0.001822 \pm 0.000035$	$+0.00050 \pm 0.00016$
A_2	$(-1.40 \pm 0.13)\times10^{-5}$	------
B_2	$(-0.97 \pm 0.15)\times10^{-5}$	$(-0.3 \pm 0.7)\times10^{-5}$
$\|R_v\|^2$	$(2.371 \pm 0.021)\times10^{-8}$ D^2	$(4.61 \pm 0.07)\times10^{-8}$ D^2
S^o_v	$(47.6 \pm 0.4)\times10^{-24}$	$(3.60 \pm 0.05)\times10^{-24}$
S_{Band}	$(47.2 \pm 0.4)\times10^{-24}$	$(3.61 \pm 0.05)\times10^{-24}$

* $|R_v|^2$ is the rotationless transition moment squared for $^{12}C^{16}O_2$ in units of $Debye^2$. The A_1 and A_2 Herman-Wallis parameters are dimensionless. The units of S^o_v are $cm^{-1}/(molecule/cm^2)$ at 296 K.

TABLE 9. Intensity Parameters for the 5349, 5248, and 5218 cm^{-1} Bands of $^{12}C^{16}O_2$.

Parameter*	$(10^02)_I \leftarrow (01^10)_I$	$(10^02)_{II} \leftarrow (01^10)_I$	$(30^01)_I \leftarrow (10^00)_{II}$
ν_o	5349.310 cm^{-1}	5247.832 cm^{-1}	5217.673 cm^{-1}
$\|R_v\|$	$(8.06 \pm 0.20)\times10^{-5}$	$(13.27 \pm 0.19)\times10^{-5}$	$(77.35 \pm 0.53)\times10^{-5}$
A_1	$(-2.87 \pm 0.09)\times10^{-2}$	$(+1.45 \pm 0.04)\times10^{-2}$	$(+3.6 \pm 1.5)\times10^{-4}$
A_2	----------	----------	$(-5.4 \pm 1.3)\times10^{-5}$
B_2	$(3.2 \pm 2.4)\times10^{-5}$	$(-3.2 \pm 1.5)\times10^{-5}$	----------
$\|R_v\|^2$	$(6.50 \pm 0.32)\times10^{-9}$	$(1.76 \pm 0.05)\times10^{-8}$	$(5.98 \pm 0.08)\times10^{-7}$ D^2
S^o_v	$(0.512 \pm 0.025)\times10^{-24}$	$(1.36 \pm 0.04)\times10^{-24}$	$(2.279 \pm 0.031)\times10^{-24}$
S_{Band}	$(0.630 \pm 0.031)\times10^{-24}$	$(1.42 \pm 0.04)\times10^{-24}$	$(2.153 \pm 0.030)\times10^{-24}$

* $|R_v|^2$ is the rotationless transition moment squared for $^{12}C^{16}O_2$ in units of $Debye^2$. The A_1, A_2 and B_2 Herman-Wallis parameters are dimensionless. The units of S^o_v and S_{Band} are $cm^{-1}/(molecule/cm^2)$ at 296 K.

FIGURE CAPTIONS

Fig. 1. Region of the Q Branch of the $(01^12)_I \leftarrow (00^00)_I$ band on spectrum #7. In addition to the P-, Q-, and R-Branch lines of the ground state band, lines from two of its hot bands, $(02^22)_I \leftarrow (01^10)_I$ and $(10^02)_I \leftarrow (01^10)_I$, are indicated on the spectrum. Water lines formed in the air-path between the White cell and the FTS are indicated by the ◊ symbol. The strongest of these water lines obscures the P10 and Q40 lines of the $(01^12)_I \leftarrow (00^00)_I$ CO_2 band.

Fig. 2. Region of the Q Branch of the $(02^22)_I \leftarrow (01^10)_I$ band on spectrum #6. Water lines are indicated by the ◊ symbol. The strong CO_2 lines belong to the P branch of the $(01^12)_I \leftarrow (00^00)_I$ band. The strongest water line obscures the Q12 and Q13 lines, and the P28 line of the $(01^12)_I \leftarrow (00^00)_I$ band obscures the Q16 and Q17 lines of the $(02^22)_I \leftarrow (01^10)_I$ band. Q35 also cannot be measured.

Fig. 3. Line intensities measured for the $(01^12)_I \leftarrow (00^00)_I$ band, shown at their wavenumber positions. The ◊ symbol is used for the P and R branches, and the • symbol is used for the Q branch.

Fig. 4. Weighted quadratic least-squares fit of $[S_{red}]^{0.5}$ to Eq. 5 for the $(01^12)_I \leftarrow (00^00)_I$ band P and R branches to determine $|R_v|$, A_1 and A_2. $|R_v|$ was determined simultaneously with the fit of the Q branch measurements of $[S_{red}]^{0.5}$ to Eq. 6.

Fig. 5. Weighted least-squares fit of $[S_{red}]^{0.5}$ vs J''^2 to Eq. 6 for the $(01^12)_I \leftarrow (00^00)_I$ band Q branch to determine $|R_v|$, and B_2, done simultaneously with the fit of the P and R branch measurements to Eq. 5, as shown in Fig. 4.

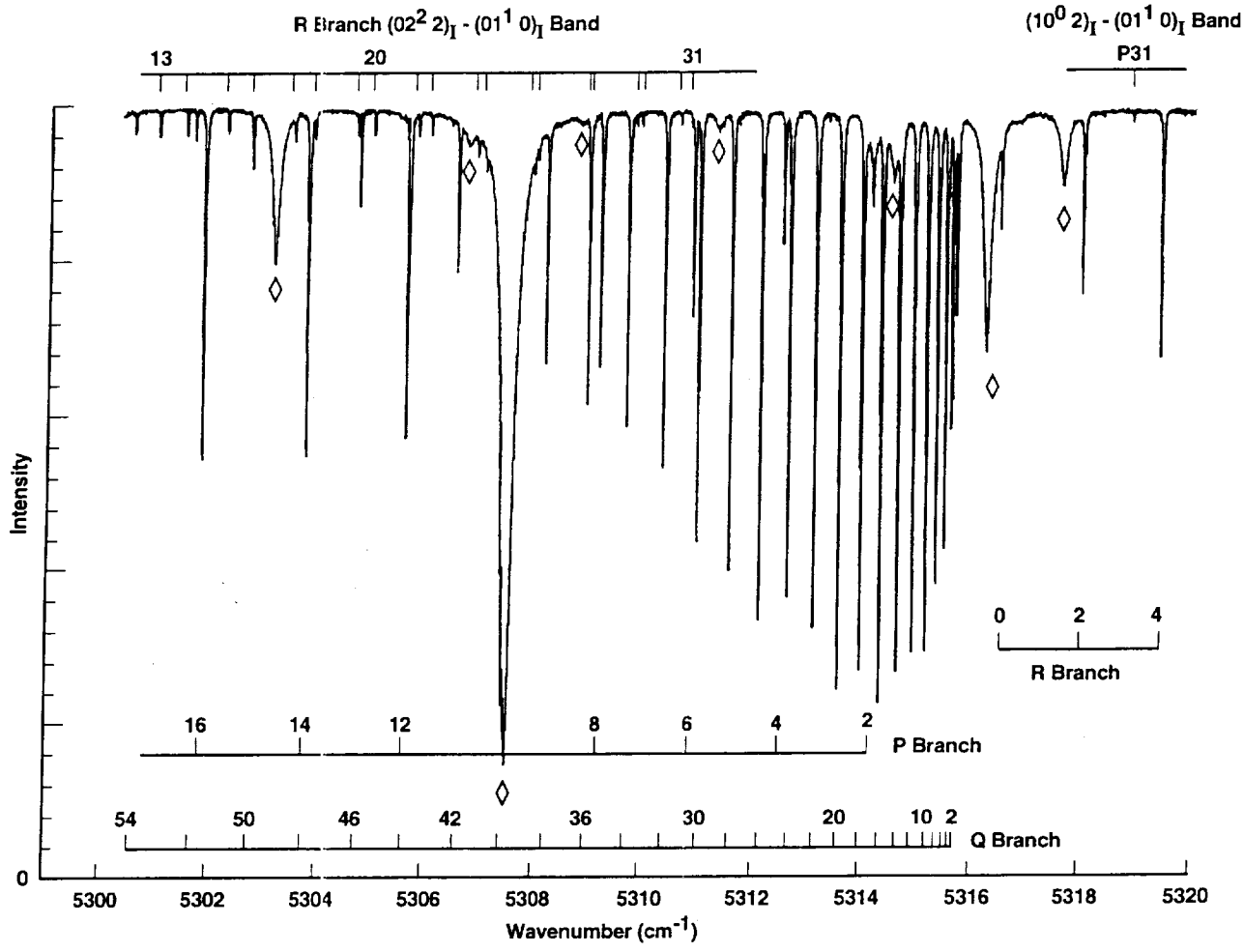
R Branch $(02^2\ 2)_I$ - $(01^1\ 0)_I$ Band
$(10^0\ 2)_I$ - $(01^1\ 0)_I$ Band
13
20
31
P31
Intensity
0
0
2
4
R Branch
16
14
12
8
6
4
2
P Branch
54
50
46
42
36
30
20
10
2
Q Branch
5300
5302
5304
5306
5308
5310
5312
5314
5316
5318
5320
Wavenumber (cm^{-1})

Giver-01

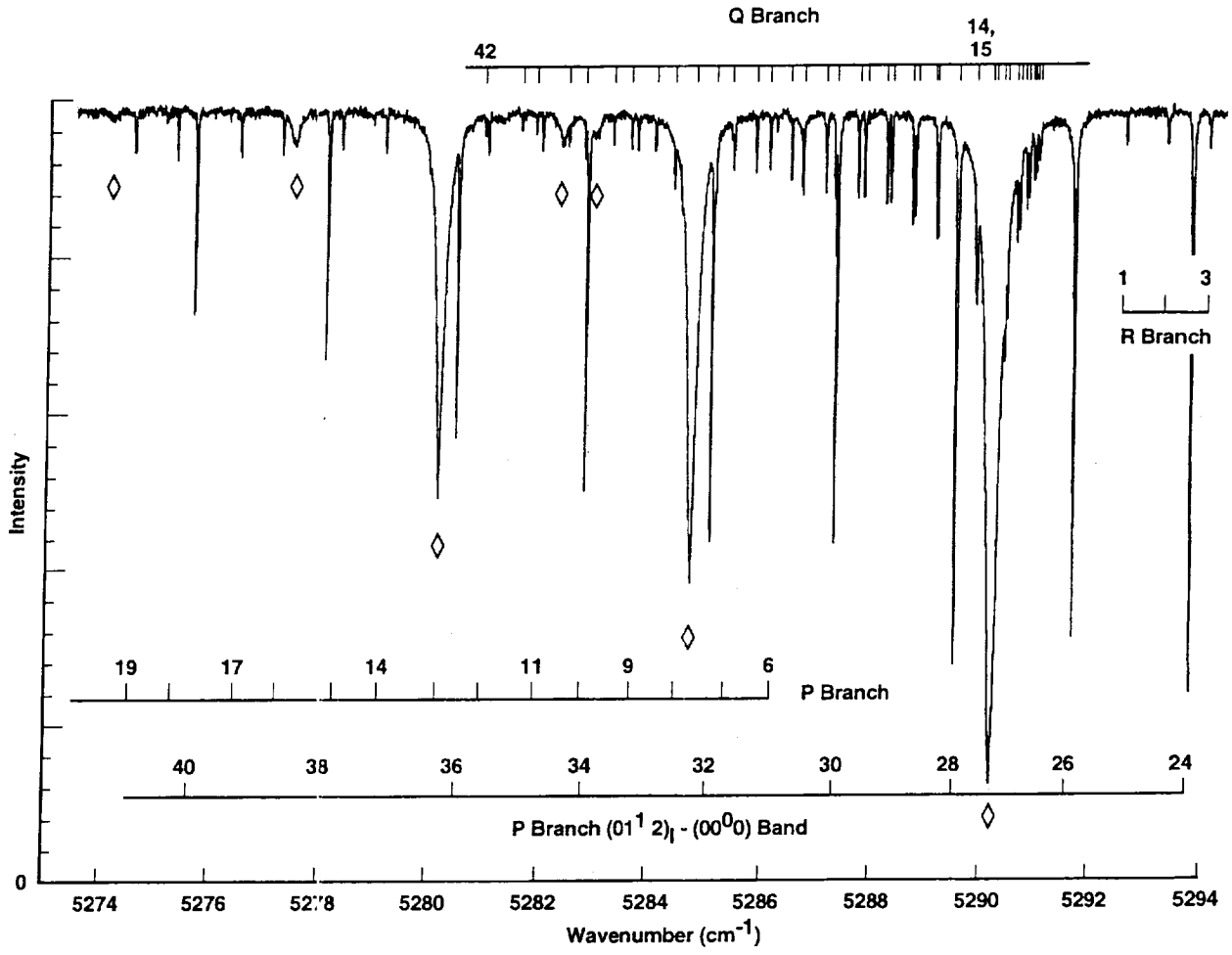
Q Branch
42
14,
15
1
3
R Branch
Intensity
19
17
14
11
9
6
P Branch
40
38
36
34
32
30
28
26
24
P Branch (01^{1} 2)$_{l}$ - (00^{0}0) Band
0
5274
5276
5278
5280
5282
5284
5286
5288
5290
5292
5294
Wavenumber (cm^{-1})

Giver-02

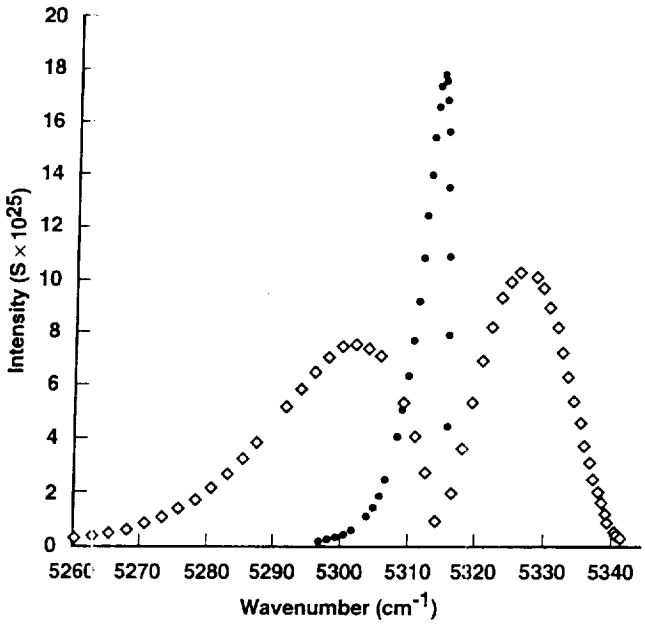
20
18
16
14
12
10
8
6
4
2
0
Intensity (S × 10^25)
5260
5270
5280
5290
5300
5310
5320
5330
5340
Wavenumber (cm^-1)

Giver-03

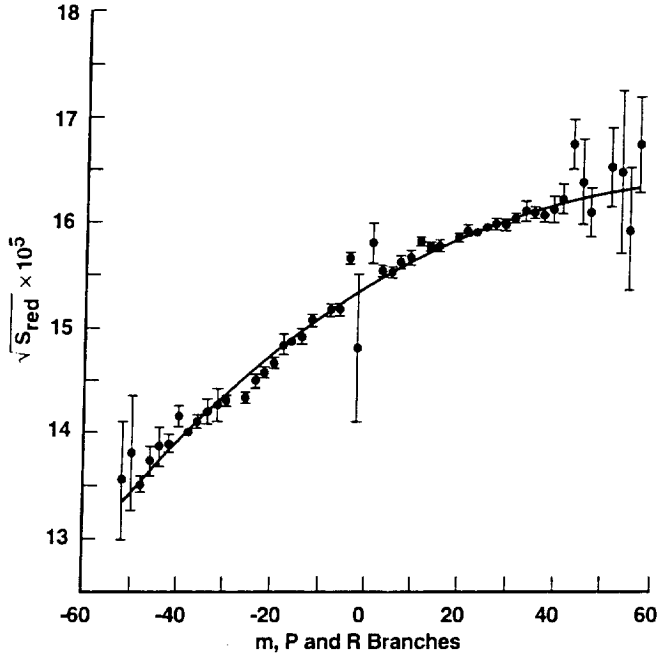
18
17
16
15
14
13
$\sqrt{S_{red}} \times 10^5$
-60
-40
-20
0
20
40
60
m, P and R Branches

Giver-04

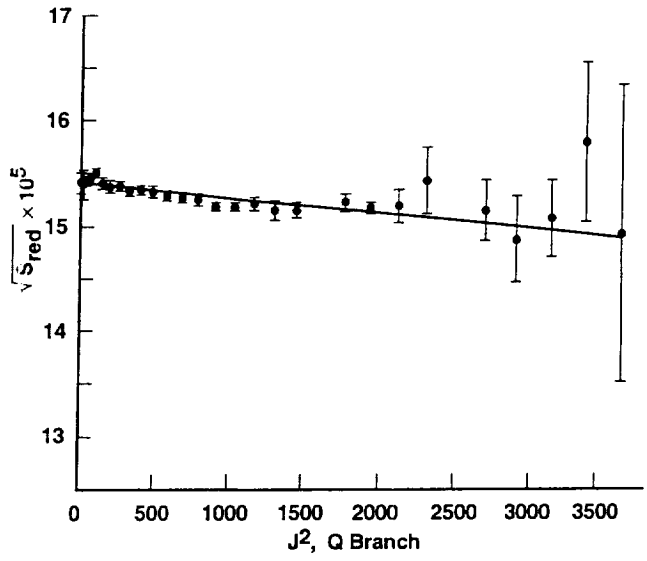
17
16
15
14
13
$\sqrt{S_{red}} \times 10^5$
0
500
1000
1500
2000
2500
3000
3500
J^2, Q Branch

Giver-05